Widespread Telomere Instability in Prostatic Lesions

LiRen Tu,[1] Nazmul Huda,[1] Brenda R. Grimes,[1] Roger B. Slee,[1] Alison M. Bates,[1] Liang Cheng,[2] and David Gilley[1]*

[1]*Department of Medical and Molecular Genetics, Indiana University School of Medicine, Indianapolis, Indiana*
[2]*Department of Pathology and Laboratory Medicine, Indiana University School of Medicine, Indianapolis, Indiana*

A critical function of the telomere is to disguise chromosome ends from cellular recognition as double strand breaks, thereby preventing aberrant chromosome fusion events. Such chromosome end-to-end fusions are known to initiate genomic instability via breakage-fusion-bridge cycles. Telomere dysfunction and other forms of genomic assault likely result in misregulation of genes involved in growth control, cell death, and senescence pathways, lowering the threshold to malignancy and likely drive disease progression. Shortened telomeres and anaphase bridges have been reported in a wide variety of early precursor and malignant cancer lesions including those of the prostate. These findings are being extended using methods for the analysis of telomere fusions (decisive genetic markers for telomere dysfunction) specifically within human tissue DNA. Here we report that benign prostatic hyperplasia (BPH), high-grade prostatic intraepithelial neoplasia (PIN), and prostate cancer (PCa) prostate lesions all contain similarly high frequencies of telomere fusions and anaphase bridges. Tumor-adjacent, histologically normal prostate tissue generally did not contain telomere fusions or anaphase bridges as compared to matched PCa tissues. However, we found relatively high levels of telomerase activity in this histologically normal tumor-adjacent tissue that was reduced but closely correlated with telomerase levels in corresponding PCa samples. Thus, we present evidence of high levels of telomere dysfunction in BPH, an established early precursor (PIN) and prostate cancer lesions but not generally in tumor adjacent normal tissue. Our results suggest that telomere dysfunction may be a common gateway event leading to genomic instability in prostate tumorigenesis.

Key words: telomere dysfunction; genomic instability; benign prostatic hyperplasia; prostatic intraepithelial neoplasia; prostate cancer

INTRODUCTION

The telomere, a complex of tandem (T_2AG_3) DNA repeats and associated proteins, disguises the chromosome terminus from recognition as a double strand break and inhibits linkage events with other genomic regions. Telomeric DNA sequences are generated by telomerase, a reverse transcriptase that utilizes an internal RNA moiety and a protein catalytic subunit known as hTERT [1,2]. Telomerase activity is present in normal primitive cellular subpopulations (i.e., progenitor cells), germ line cells, and in the majority of premalignant and malignant lesions but is generally not present at sufficient levels in normal somatic cells to maintain telomere length [2–4].

Critically shortened telomere lengths normally trigger tumor suppression via senescence and apoptotic pathways [3,5]. However, these tumor suppressive mechanisms may be disrupted in a rare cell or small groups of cells by telomere dysfunction and other forms of genomic instability lowering the threshold of cancer initiation and progression [3,5,6]. In addition, chromosome end-to-end fusions with subsequent stochastic breakage-fusion-bridge cycles may contribute to the intratumoral genomic heterogeneity reported in many human cancers [6–8].

Multiple types of lesions of varying morphological characteristics and severity can afflict the prostate. High-grade prostatic intraepithelial neoplasia (PIN) has been identified as a likely precursor lesion to PCa [9]. PIN has been shown to share similar molecular profiles and cytogenetic aberrations as PCa and has been localized to the same epithelial layers and prostatic tissue compartments [9–11]. In PIN, the basal epithelial layer begins to disappear as the secretory cells proliferate, and in PCa the basal epithelial layer vanishes entirely, indicating a likely progression from PIN to PCa [11].

Abbreviations: BPH, benign prostatic hyperplasia; Cp, crossing point; FGFR1, fibroblast growth factor receptor 1; H&E, Haematoxyl Eosin; HPN, hepsin; IGF2, insulin-like growth factor 2; PCa, prostate cancer; PIN, prostatic intraepithelial neoplasia; PSA, prostate specific antigen; PTEN, phosphatase and tensin homologue; TBP, TATA-box-binding protein; TRAP, telomeric repeat amplification protocol; TGFß3, transforming growth factor beta 3.

LiRen Tu and Nazmul Huda contributed equally to this work.

Conflict of interest: Authors declare no competing interest.

*Correspondence to: Department of Medical and Molecular Genetics, Indiana University School of Medicine, 975 West Walnut Street, IB-244B, Indianapolis, IN.

Received 10 October 2014; Revised 13 February 2015; Accepted 26 March 2015

DOI 10.1002/mc.22326

Published online in Wiley Online Library (wileyonlinelibrary.com).

Another highly prevalent type of prostatic lesion called benign prostatic hyperplasia (BPH) is characterized by excessive proliferation of prostatic cells and results in severe urinary tract complications in a large percentage of older males [12,13]. A predominant model of BPH, which originates in basal epithelial cells, is that it does not progress to PCa, as its name implies [14–16]. However, several recent reports indicate that BPH and PCa may share more similarities than previously identified. Mapping of prostatic carcinomas to their regions of origin showed that 25% were derived from the transition zone, traditionally believed to be the exclusive site of BPH, and two thirds of the transition zone carcinomas were found concomitantly with BPH in the same region, thus preventing a clear distinction between the two types of lesions based on prostate location [17]. Furthermore, BPH and PCa share some gene expression profiles involved in cancer development and progression, and both express telomerase [17–22]. Though several large-scale epidemiological studies indicate that men with BPH have an increased risk of prostate cancer and prostate-cancer-related mortality, it remains unclear whether this association reflects a causal link [23].

Anaphase bridges have been noted along with significantly shortened telomeres in multiple types of human cancer cells [5]. These findings are now being extended using methods for the analysis of telomere fusion in human cancers. Telomere fusions are a decisive genetic marker for telomere dysfunction. Reports of telomere fusions in leukemia and solid tumors (colon and breast) have added increasing support to the hypothesis that telomere dysfunction plays a critical role in the development of genomic instability and tumorigenesis [24–26].

Here, we report that BPH, PIN, and PCa samples revealed similarly high frequencies of telomere fusions and anaphase bridges. In addition, the majority of BPH, PIN, and PCa tissues exhibited telomerase activity, though PCa tissues on average contained the highest levels of telomerase. Additionally, tumor-adjacent, histologically normal prostate tissue did not generally contain telomere fusions (1 of 15 were positive for telomere fusions) but surprisingly exhibited levels of telomerase activity reduced but comparable to matched PCa tissue. Furthermore, telomere length was found to be the shortest in PCa samples and was significantly shorter in PCa samples than in matched tumor adjacent, histologically normal tissues. These results indicate that telomere dysfunction is a highly prevalent genetic aberration present in hyperplasic to neoplastic prostatic lesions.

MATERIALS AND METHOD

Cell Lines

Human foreskin fibroblast BJ, BJ E6/E7 cells were kindly provided by Dr. Woodring Wright (University of Texas Southwestern Medical Center) [27]. HeLa cells were purchased from the American Type Culture Collection (http://www.atcc.org/), which were tested and authenticated by the cell bank using their standard short tendem repeats (STR)-based techniques. All cells were continuously monitored microscopically to ascertain conformity to the appropriate in vitro morphologic characteristics. Cells were additionally checked to be free of mycoplasma contamination. Cells were cultured in advanced DMEM (Life Technologies, Grand Island, NY) with L-glutamine, penicillin-streptomycin, and 5% FBS at 37°C in 5% (vol/vol) carbon dioxide.

Prostate Tissues

Human prostate tissues with BPH (30; age range 53–90; mean 69.4), high-grade PIN (24; age range 55–71; mean 63.7), PCa (32; age range 49–76; mean 62.3), and adjacent normal (15; age range 49–76; mean 62.9) were obtained from the Indiana University Simon Cancer Center Tissue Bank (Table 1 and Figure 1A). Adjacent normal tissues were surgically removed at least 5 mm from the closest surgical resection margins of all prostatic lesions [28,29]. BPH tissue was obtained from patients who underwent transurethral resection for BPH treatment. High grade PIN, PCa, and adjacent normal tissue were obtained from radical prostatectomy specimens from prostate cancer patients. Each aliquot of de-identified tumor tissue was given a unique barcode for identification. The lesions were histologically confirmed by a urologic pathologist (L.C.). This research was approved by the Indiana University School of Medicine Institutional Review Board.

mRNA Assays for Signature Genes

mRNA steady-state levels of several genes (HPN, PSA, MYC, TP53, IGF2, FGFR1, TGFB3, and PTEN) were determine by real-time PCR from BPH, PIN, and PCa prostatic tissue lesions. cDNA was generated from Trizol extracts using the Quantiscript Reverse Transcriptase Fastlane cDNA kit (Qiagen, Valencia, CA). Samples were subjected in triplicate to 40 amplification cycles (10 s at 95°C, 20 s at 60°C, and 30 s at 72°C) on the LightCycler® 480 II (Roche, Indianapolis, IN). The negative controls used were (i) no cDNA template, and (ii) no reverse transcription treatment in each experiment. Gene transcript levels were calculated utilizing the ΔΔCt method [30] with TBP (TATA box binding protein) expression as a loading control. The primers used were: HPN_F, 5′-GATGTCTGCAATGGCGCTGAC-3′; HPN_R, 5′-CCACACAGCCGCCAACGTG-3′; PSA_F, 5′-GGCATCAGGAACAAAAGCGTGA-3′; PSA_R, 5′-CCTGAGGCGTAGCAGGTGGTCCCCAG-3′; MYC_F, 5′-TAC CCT CTC AAC GAC AGC AG-3′; MYC_R, 5′-TCT TGA CAT TCT CCT CGG TG-3′; TP53_F, 5′-GCCATCTACAAGCAGTCACAGCACAT-3′; TP53_R, 5′-GGCACAAACACGCACCTCAAAGC-3′; IGF2_F, 5′-GCACA-

Table 1. Benign prostatic hyperplasia, high-grade prostatic intraepithelial neoplasia, and prostate cancer tissues

BHP		PIN		PCa				
Type	Age	Type	Age	Type	Age	Gleason	T	N
BHP	53	PIN	55	PCa	49	3 + 4 = 7	T3a	N0
BHP	56	PIN	56	PCa	49	3 + 4 = 7	T3b	N1
BHP*	56	PIN	58	PCa†	51	4 + 3 = 7	T3a	N1
BHP	57	PIN	58	PCa	52	3 + 4 = 7	T3a	N0
BHP	57	PIN	60	PCa	54	3 + 4 = 7	T3a	N0
BHP	58	PIN	60	PCa†	56	3 + 4 = 7	T2a	N0
BHP	60	PIN	61	PCa†	56	4 + 3 = 7	T3a	N0
BHP*	62	PIN	61	PCa	57	3 + 4 = 7	T3a	N.A.
BHP	64	PIN	62	PCa	58	3 + 4 = 7	T3a	N0
BHP*	65	PIN	64	PCa†	58	3 + 4 = 7	T2b	N0
BHP	66	PIN	65	PCa	60	3 + 4 = 7	T3a	N0
BHP*	66	PIN	65	PCa†	61	3 + 3 = 6	T2a	N.A.
BHP	67	PIN	66	PCa†	61	3 + 3 = 6	T2b	N0
BHP	71	PIN	66	PCa	62	4 + 3 = 7	T3b	N.A.
BHP	71	PIN	66	PCa	63	4 + 3 = 7	T3b	N1
BHP	71	PIN	66	PCa†	63	3 + 4 = 7	T3a	N0
BHP	73	PIN	67	PCa†	63	3 + 3 = 6	T2b	N0
BHP	74	PIN	67	PCa	64	4 + 3 = 7	T3b	N1
BHP	74	PIN	69	PCa	64	4 + 3 = 7	T2b	N0
BHP*	74	PIN	69	PCa†	64	3 + 3 = 6	T2c	N.A.
BHP*	74	PIN	70	PCa	64	3 + 3 = 6	T2c	N.A.
BHP	75	PIN	71	PCa†	65	3 + 4 = 7	T2b	N.A.
BHP*	75	PIN	NA	PCa	67	4 + 3 = 7	T2b	N0
BHP*	75	PIN	NA	PCa†	68	4 + 3 = 7	T3b	N.A.
BHP	76			PCa	68	5 + 4 = 9	T3b	N0
BHP*	76			PCa†	69	4 + 5 = 9	T3a	N.A.
BHP	79			PCa	71	3 + 4 = 7	T3a	N0
BHP*	82			PCa	71	4 + 3 = 7	T3a	N1
BHP	84			PCa‡	72	3 + 3 = 6	T2b	N0
BHP	90			PCa†	74	4 + 3 = 7	T3a	N0
				PCa	76	3 + 4 = 7	T2c	N0
				PCa†	NA	3 + 4 = 7	T3a	N.A.

BPH, benign prostatic hyperplasia; PCa, prostate cancer; N.A., not available; PIN, prostate intraepithelial neoplasia.
*Matching blood collected.
†Tumor adjacent, histologically normal tissue collected.
‡Only tumor adjacent, histo;ogically normal tissue collected.

GCAGCATCTTCAAAC-3′; IGF2-R, 5′- TTGGTCTTACTGGGTCCCTC-3′; FGFR1_F, 5′-ATCATCTATTGCACAGGGGCC-3′; FGFR1_R, 5′-CATACTCAGAGACCCCTGCTAGC-3′; TGFβ3_F, 5′-CACCCAGGAAAACACCGAGTC-3′; TGFβ3_R, 5′-CTCATTGTCCCACGCCTTTGAA-3′; PTEN_F, 5′-GTTTACCGGCAGCATCAAAT-3′ and PTEN_R, 5′-CCCCCACTTTAGTGCACAGT-3′.

TAR Fusion PCR

Genomic DNA was isolated from all prostate tissues using the DNeasy Tissue Kit (Qiagen, MD). TAR fusion PCR was performed following the protocol described previously [26]. Two-step touchdown PCRs were performed in a 20 μl reaction mixture using 50 ng of DNA, multiple primers, 10% 7-deaza-dGTP (Roche Diagnostics), and Advantage GC Genomic LA Polymerase Mix (Clontech Laboratories, Inc.,). The cycling conditions were initial denatured at 94°C for 3 min followed by 10 cycles of 94°C for 30 s, and 72°C (−0.4°C each cycle to a "touchdown" at 68°C) for 5 min, and then 20 cycles of 94°C for 30 s, 68°C for 5 min. Primer mix A contained eight primers that anneal within TAR1 regions (with the exception of Xp and 17p): 1p, 2p, 5p, 7q, 9p, 11q, 12q, 15q, 16p, 17p, 18p, Xp, and Xq. Primer mix B contained eight primers that anneal within TAR1 regions (with the exception of Xp and 17p): 1q, 2p, 4p, 4q, 5p, 7q, 10q, 12q, 17p, 18p, 19q, 21q, and Xp. Primer sequences have been described previously [26]. TAR Fusion PCR products were then resolved on a 0.8% agarose gel and Southern analysis was performed using a ^{32}P-labeled $[TTAGGG]_4$ probe. To calculate the total number of possible telomere fusion combinations, the general equation $C(n,2)+n$ was used, where n is the number of unique chromosomal ends. This equation can be simplified to $n(n+1)/2$. In human somatic cells with 46 possible unique chromosome ends, there are

A

Type	Sample size	Age range	Mean	Median
BPH	30	53-90	69.3	71
PIN	24	55-71	63.7	65
PCa	32	49-76	62.2	63
Adjacent	15	49-76	63	63

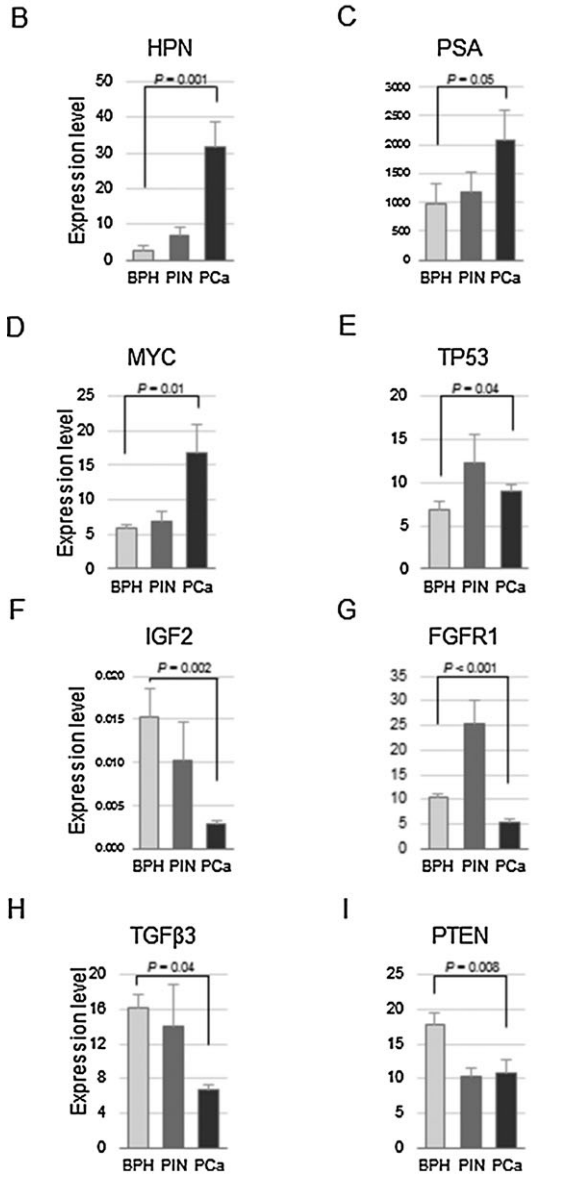

Figure 1. Patient age and selected gene expression profile. (A) Patient age ranges for benign prostatic hyperplasia (BPH), prostatic intraepithelial neoplasia (PIN), and prostate cancer (PCa) lesions described in Table 1. Comparison between BPH and PCa expression levels of HPN (B), PSA (C), MYC (D), TP53 (E), IGF2 (F), FGFR1 (G), TGFB3 (H), and PTEN (I). TATA-binding protein (TBP) was used as a normalizing control. Each bar represents the results of five to six independent samples, each with three technique replicates (mean ± se). Standard *t*-test analysis is shown.

$(46 \times 47)/2 = 1081$ possible end-to-end fusion combinations. Each primer mix covers 13 chromosome ends ($n = 13$), so each primer mix can detect $(13 \times 14)/2 = 91$ possible fusion combinations. Primer Mix A and Primer Mix B share seven primers for a total number of $(7 \times 8)/2 = 28$ shared fusion combinations. Thus, the total number of possible fusion combinations detected by both primer mixes is $91 + 91 - 28 = 154$, for a total percentage of coverage of $154/1081 = 14.2\%$

Telomere Length

Telomere length in isolated genomic DNA from prostate tissues was determined using the terminal restriction fragment length assay described elsewhere [31].

Telomerase Activity

Telomerase activity assay was performed by the telomeric repeat amplification protocol (TRAP) using the TRAPeze Telomerase Detection Kit (Millipore, MA). Tissues (approx. 10 mg each) were lysed with ice-cold 1 × CHAPS lysis buffer [10 mM Tris-HCl (pH 7.5), 1 mM $MgCl_2$, 1 mM EGTA, 0.1 mM benzamidine, 5 mM β-mercaptoethanol, 0.5% CHAPS, and 10% glycerol] containing RNase inhibitor at a final concentration of 100 U/mL. A reaction mixture of 50 μl containing 0.5 μg of protein extract, 10 μl of 5 × TRAP reaction mix (Tris buffer, primers, dNTPs, and oligomer mix for amplification of 36-bp internal control band), and 2 U of Taq DNA polymerase were incubated for 30 min at 30°C and then subjected to denaturation at 95°C for 5 min. A PCR of 30 cycles of 95°C for 30 s, 52°C for 30 s, and 72°C for 30 s was performed. For direct visualization of the TRAP ladders, the PCR products were electrophoresed on a 12.0% polyacrylamide gel and and visualized by SYBR Green phosphorimaging, as described [32].

hTERT mRNA Levels

Total cellular RNA was extracted from 5–10 mg of tumour tissues using the RNeasy Mini isolation kit (Qiagen, Hilden, Germany) according to the manufacturer's protocol. The cDNA was generated from total RNA using the Quantiscript Reverse Transcriptase Fastlane cDNA kit (Qiagen, Valencia, CA). The quantitative real-time PCR of hTERT and TATA-box-binding protein (TBP) (as an internal control) were performed on the LightCycler® 480 II (Roche). The hTERT primer sequences were 5′-CGG TGT GCA CCA ACA TCT AC-3′ (forward) and 5′-CAC ACA TGC GTG AAA CCT G-3′ (reverse), and hTERT probe was Probe #18 from Universal ProbeLibrary (Roche). TBP primers and probe were from Universal ProbeLibrary Human TBP Gene Assay (Roche), and the primer sequences were 5′-TGA ATC TTG GTT GTA AAC TTG ACC-3′ (forward) and 5′-CTC ATG ATT ACC GCA GCA AA-3′ (reverse). The reaction mix was incubated at 95°C for 10 min, and 45 cycles of PCR at 95°C for 10 s, 60°C for

30 s, and 72°C for 1 s, followed by cooling to 40°C. The hTERT signal was detected by filter FAM (465–510 nm), and TBP by filter HEX/Yellow555 (533–580 nm). All samples were measured in triplicate. The crossing point (Cp) was determined by the second derivative maximum method, and hTERT mRNA level was expressed as a ratio of hTERT to TBP cDNA amount in respective subpopulations as well as in HeLa positive control determined by "Advanced Relative Quantification" using Light Cycler® 480 Software (1.5.0, Roche).

Fluorescence In Situ Hybridization

Fluorescence in situ hybridization was performed on isolated nuclei following the method described previously [33]. FISH probes were commercial CEP 17 (Spectrum Green), CEP X (Spectrum Green and Orange), and CEP Y (Spectrum Orange) (Abbott Molecular, Des Plaines, IL). DAPI stained images were captured at $\times 100$ magnification using a Spot RTKE camera (Diagnostic Instruments, Sterling Heights, MI), mounted on a Leica DN5000B microscope (Leica Microsystems, Buffalo Grove, IL). More than 50 nuclei were scored per sample.

Analysis of Anaphase Bridges

Haematoxyl Eosin (H&E) stained tissue sections of human prostate lesion tissues (BPH, PIN, and PCa) were received from the Indiana University Simon Cancer Center Tissue Bank with Indiana University School of Medicine Institutional Review Board approval. The slides were histologically confirmed by a urologic pathologist (LC). Anaphase bridges in H&E stained tissues of BPH, PIN, and PCa with corresponding adjacent, histologically normal prostate tissues were quantitated microscopically (Leica DN5000B) [34,35]. An anaphase bridge was defined as a continuous chromatin link between the two separated chromosome masses at anaphase [36].

Statistical Analysis

Statistical significance was calculated using the Student's *t*-test. A difference of $P < 0.05$ was considered statistically significant.

RESULTS

Prostate tissue specimens were obtained and reviewed for histological confirmation by a urological pathologist (LC) at the Indiana University Simon Cancer Center (Table 1 and Figure 1A). In addition, mRNA expression assays were performed for specific genes previously associated with BPH and PCa [hepsin (HPN), prostate specific antigen (PSA), c-Myc oncogene, TP53, insulin-like growth factor 2 (IGF2), fibroblast growth factor receptor 1 (FGFR1), transforming growth factor beta 3 (TGFβ3), and phosphatase and tensin homologue (PTEN)]. Of these eight genes, expression of HPN [37–40], PSA [38,41], MYC [37,39,42], and TP53 [41,43–46] was significantly higher in PCa than in BPH, while expression of IGF2 [37,38,40,47], FGFR1[38,47], TGFβ3 [38,47,48], and PTEN [42] was significantly downregulated in PCa compared to BPH as previously reported (Figure 1B–I). Additionally, we compared the expression of these key signature genes with the PIN tissues used in these studies. PIN tissues exhibited significantly higher expression than BPH or PCa in TP53 and FGFR1 (Figure 1E and G). Expression of TGFβ3 and PTEN in PIN was slightly lower than in PCa and much lower than in BPH (Figure 1H and I). HPN, PSA, MYC, and IGF2, however, were expressed at intermediate levels in PIN, as compared to BPH and PCa (Figure 1B–F). Our results confirm previous reports regarding differential expression of these key signature genes for the BPH and PCa tissues used in this study.

We utilized a multiplex PCR-based assay, TAR (telomere-associated repeat) fusion PCR, to quantitate the frequencies of telomere fusions using isolated DNA from each tissue sample [26]. Telomere fusion levels are a decisive genetic marker for the extent of telomere dysfunction in DNA isolated from human tissue samples since conventional cytogenetic approaches are not feasible in this context [26]. We examined telomere fusion frequencies in genomic DNA isolated from BPH ($n = 30$), PIN ($n = 24$), PCa ($n = 31$), and tumor-adjacent, histologically normal (adjacent; #15) human prostate tissue samples. Patient ages ranged from 49 to 90, with an overall mean age of 65 (Figure 1A). All three types of prostatic lesions examined contain similarly high frequencies of telomere fusions (BPH = 65%; PIN = 55%; PCa = 62%; Figure 2) particularly considering the current limitation of chromosome fusion coverage (see Materials and Method section "TAR fusion PCR" for explanation). No fusions were observed in white blood cell DNA isolated from 10 matched BPH patients (Table 1 and Figure 2) and only 1 of 15 tumor-adjacent, histologically "normal" tissues from matched PCa patients contained detectable levels of telomere fusions (Figure 1A and Figure 2). The presence of telomere fusions in the three prostatic lesions tested was not correlated with increasing patient age and corresponding normal adjacent tissues generally did not contain telomere fusions regardless of patient age. These results indicate that high frequencies of telomere fusions are a common feature of all three types of prostatic lesions: BPH, PIN, and PCa prostate tissue.

Telomere dysfunction has been suggested to cause aneuploidy as a result of subsequent breakage-fusion-bridge cycles [6], and aneuploidy states of specific chromosomes have previously been reported for all three types of prostatic lesions examined in this study: BPH, PIN, and PCa [13,49]. To confirm the status of aneuploidy for specific chromosomes in the prostatic lesions studied here, we examined the complement of

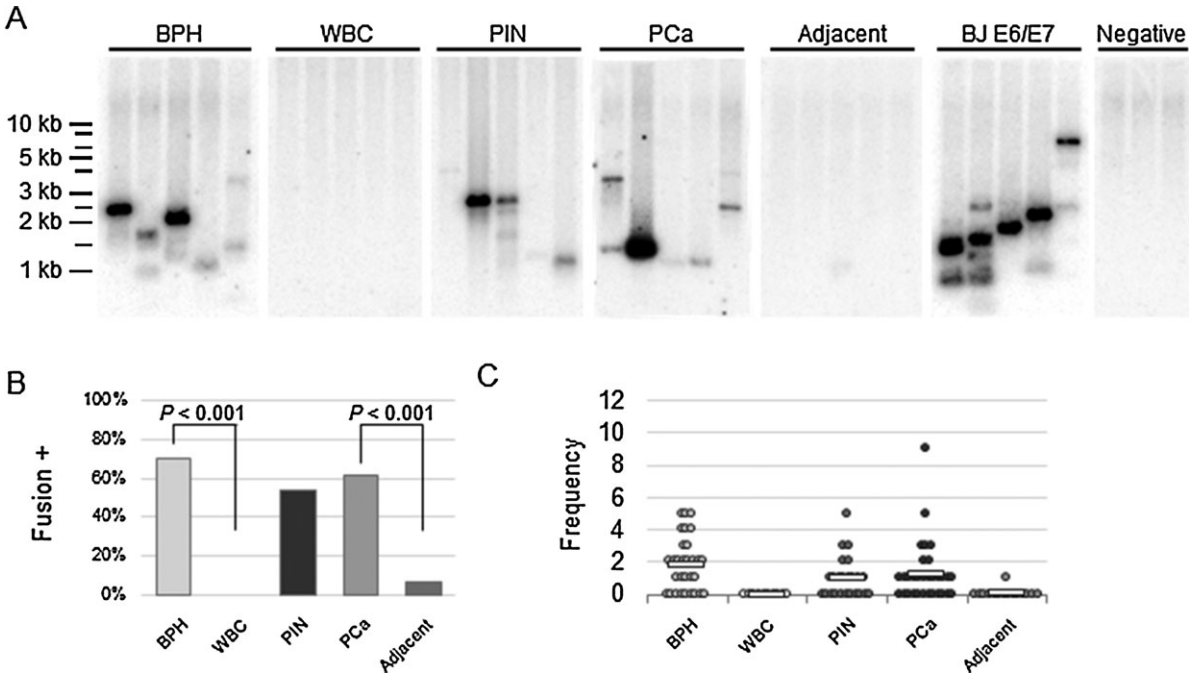

Figure 2. Telomere fusions in the prostatic lesion samples. (A) Southern blot analysis of TAR-fusion PCR products using a ^{32}P-labeled $[TTAGGG]_4$ probe. Benign prostatic hyperplasia (BPH), prostatic intraepithelial neoplasia (PIN), prostate cancer (PCa), and tumor adjacent, histologically normal adjacent (adjacent) prostate tissues. Five representative samples are shown for each sample type; BPH, white blood cells from 10 BPH patients (WBC), PIN, PCa, corresponding normal adjacent tissues from PCa patients (Adjacent), commercial human male DNA (Promega, WI) used as a negative control. BJ cultured human male foreskin fibroblast-expressing HPV16 E6/E7 (BJ E6/E7) used as a positive control for telomere fusions [27]. (B) The percentage of fusion-positive samples. Standard *t*-test analysis is shown. (C) Frequency of telomere fusions. Each dot represented one individual with the number of telomere fusion Southern bands per 500 ng genomic DNA from five TAR-Fusion PCRs.

chromosomes X and Y in BPH cells and chromosomes 17 and X in PIN, PCa, tumor-adjacent, histologically normal prostate tissue using centromere FISH probes (Figure 3). With the limited chromosomes analyzed here based on previous reports [13], all three prostatic lesions examined, BPH, PIN, and PCa, displayed levels of aneuploidy (Figure 3). Tumor adjacent, histologically normal prostate cells displayed reduced levels of aneuploidy compared to PIN and matched PCa tissues for chromosomes 17 and X. Therefore, we also report aneuploidy of selected chromosomes in BPH, PIN, and PCa tissues that is consistent with and may be in part driven by the telomere fusions reported above in these prostatic lesions.

We performed anaphase bridge analysis for each prostate lesion to determine if additional markers of genomic instability associated with telomere dysfunction were specifically detected in prostate lesion epithelial cells as opposed to other tissue cell types. We examined sectioned tissues from BPH, PIN, and PCa prostatic lesions along with corresponding adjacent normal tissue from each lesion from ten patients (Figure 4). We found that epithelial cells, but not other cell types, from all three prostatic lesion (BPH, PIN, and PCa) contain comparable levels of anaphase bridges (Figure 4B). Corresponding normal adjacent tissue from each prostatic lesion did not contain detectable levels of anaphase bridges. These results provide an additional marker for genomic instability (anaphase bridges) within BPH, PIN, and PCa tissues and suggest that prostatic epithelial cells may be the cell type of origin of other forms of genomic instability reported above (telomere fusions and aneuploidy).

To further characterize the telomere dynamics of these prostatic lesions, we analyzed hTERT mRNA and telomerase activity levels, along with telomere length (Figure 5). The majority of prostate lesion tissue samples contained detectable levels of hTERT mRNA (BPH: $11/16 = 69\%$; PIN: $9/15 = 60\%$; PCa: $15/16 = 94\%$) (Figure 5B) [20–22], and on average PCa tissue contained the highest levels of hTERT mRNA (Figure 5A). Interestingly, although adjacent tissues generally did not contain telomere fusions (Figure 2), we found detectable levels of hTERT mRNA (Adjacent: $12/14 = 86\%$) that closely correlated with hTERT mRNA levels in corresponding PCa samples (Figure 5C). The level of hTERT mRNA corresponded to the levels of telomerase activity in all prostate tissue lesions as expected from previous reports ($R^2 = 0.98$ in Figure 5D and E). Consistent with current models, PCa samples had significantly shorter telomeric DNA than the corresponding adjacent tissue samples ($P = 0.05$) (Figure 5F).

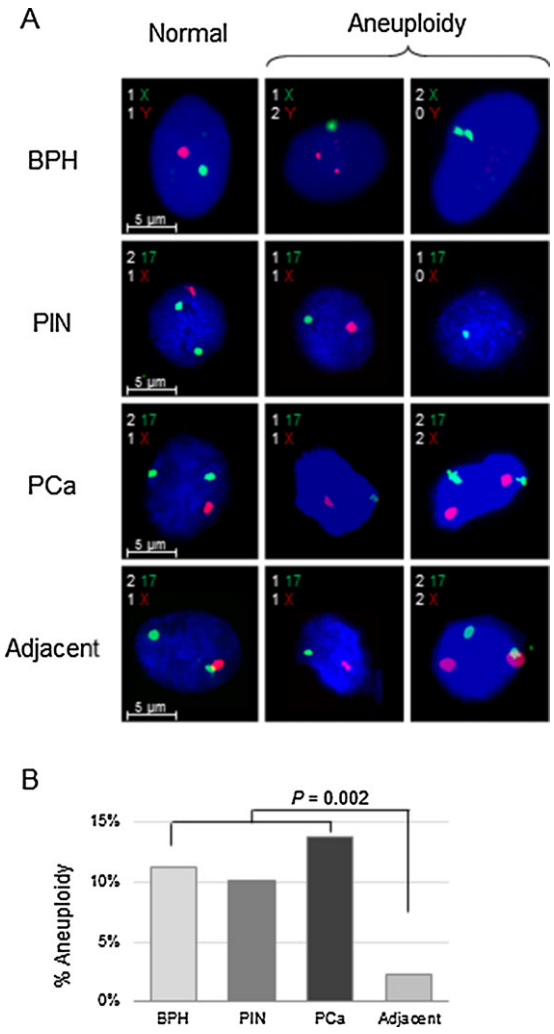

Figure 3. Detection of aneuploidy in the prostatic lesion samples. (A) Representative normal and aneuploidy centrimeric FISH images for benign prostatic hyperplasia (BPH), prostatic intraepithelial neoplasia (PIN), prostate cancer (PCa), and tumor adjacent, histologically normal adjacent (adjacent) prostate tissues. BPH was assayed for centromeres of chromosome X (green) and Y (red). The other prostate tissue types were assayed for centromeres of chromosome 17 (green) and X (red). (B) Summary of the percentage of cells carrying aneuploidy from each prostate tissue.

DISCUSSION

Here we report high frequencies of telomere fusions in PCa tumor tissues as well as in BPH and PIN prostatic lesions. These results are consistent with previous reports of telomere shortening in both pre-malignant PIN and malignant PCa cells [50–54]. The high frequency of telomere fusions in all three types of prostate lesions (BPH = 65%; PIN = 55%; PCa = 62%; Figure 2) is especially striking considering the current limitations of primer coverage in the TAR fusion PCR assay. Many distal chromosome end sequences still remain unknown, thus limiting the number of chromosome ends for which primers can be designed. The current assortment of available primers anneals to ~40% of chromosome ends, but are predicted to only amplify ~14% of the 1080 possible chromosome fusion combinations (see Materials and Method for details). We expect this to improve as technical advances are made in sequencing regions of repetitive DNA at chromosome termini. Previous reports of telomere fusion junction sequences from other cancer types indicated that no specific chromosome ends displayed a considerably higher propensity than others to form telomere fusions in spontaneous human carcinomas [24–26,55] (DG and NH, unpublished). Furthermore, the present collection of primers utilized in TAR fusion PCR were chosen solely on the basis of existing telomere-associated repeat sequences. Therefore, it is unlikely that this random assortment of primers would selectively cover certain end-to-end chromosome fusions that may be more prevalent in these prostate lesions. While the current limitations of TAR fusion PCR coverage may reduce the number of fusions detected in a sample, these constraints illustrate even more strikingly the pervasiveness of telomere fusions in the majority of these three prostatic lesions. Consequently, telomere fusion genetic markers appear to be a highly prevalent form of genomic instability that is likely present in the vast majority of spontaneously occurring human prostate lesions.

Both PIN and BPH tissues exhibited the presence of telomerase, though generally higher levels on average were found in PCa tissues as previously reported [20–22,56,57]. This is a whole tissue level observation and does not reflect a per cell quantitative comparison between these three prostate lesions since the percentage of target cells (benign, pre-malignant, or malignant epithelial cells) to "normal" unaffected epithelial/non-epithelial cells within each tissue is not uniform from sample to sample, and between lesion type to lesion type. Generally, PIN is recognized as a precursor of prostate cancer, and our findings of telomere fusions, anaphase bridges, aneuploidy, and telomerase activity in PIN tissues support this concept [9]. However, the prevailing consensus is that BPH is benign, with little to no malignant potential. The phenomenon that BPH harbors relatively high levels of genomic instability (telomere fusions, anaphase bridges, and aneuploidy) along with telomerase activity suggests that genomic instability and telomerase activation alone are not sufficient for malignant transformation and that other barriers exist to prevent (at least the vast majority of) BPH lesions from progressing into malignancy.

We found that tumor adjacent, histologically normal tissue generally did not contain detectable levels of telomere fusions but did contain correlative relatively high levels of telomerase activity compared to matched PCa tissue. The presence of telomerase activity in tumor adjacent, histologically normal tissues may be due to infiltration of activated

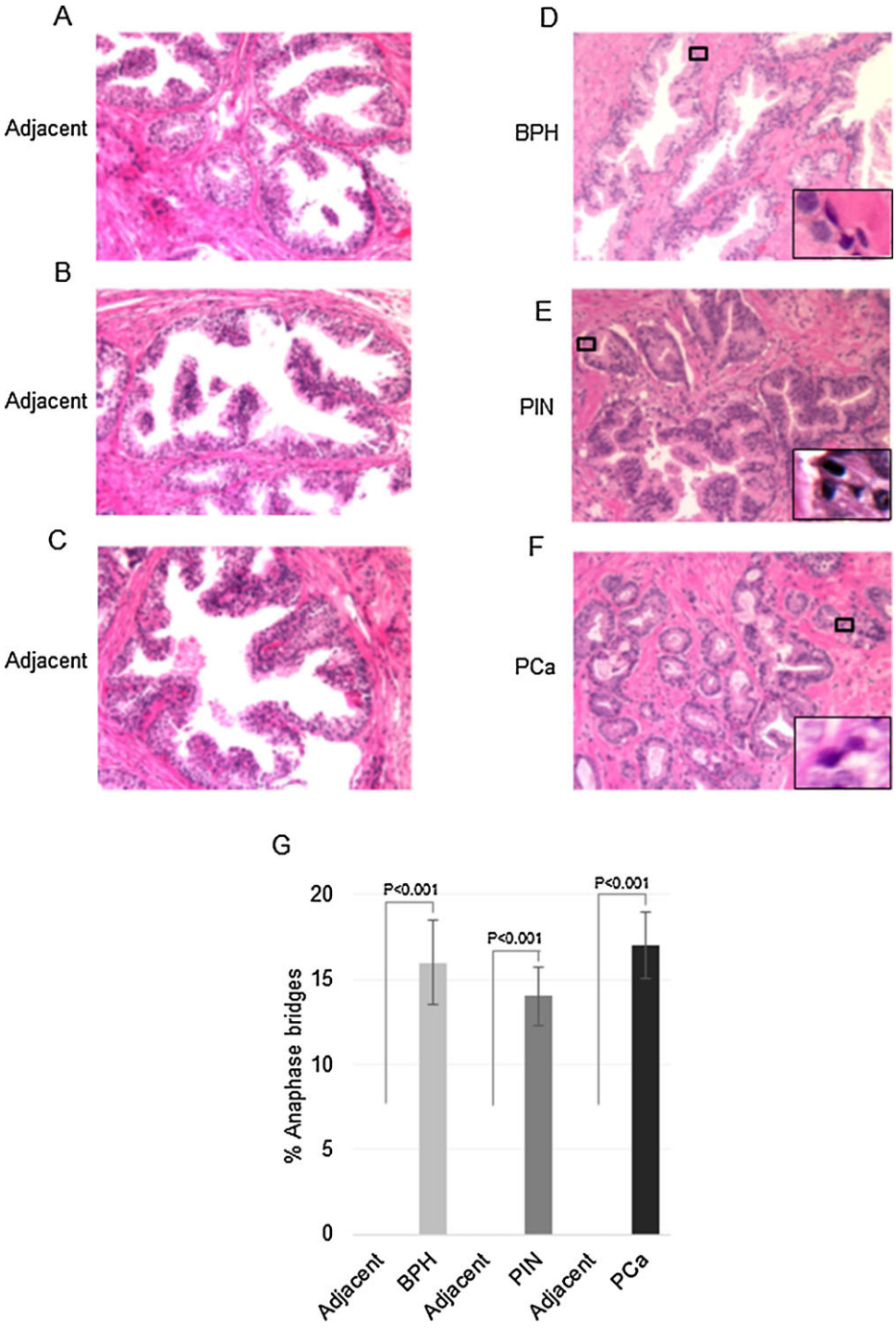

Figure 4. Anaphase bridge analysis in prostatic lesions. Tissue sections are stained with hematoxylin and eosin (H&E). (A), (B), and (C) are representative tissue sections of corresponding adjacent normal tissues from BPH, PIN and PCa lesions (adjacent), respectively. (D), (E), and (F) are representative tissue sections from BPH, PIN, and PCa, respectively. Black boxes within each prostatic tissue section field for BPH, PIN, and PCa are magnified within the lower right corner to display representative anaphase bridges. (G) The percent of anaphase bridges was calculated from the total anaphases within each prostatic lesion. Standard *t*-test analysis was performed.

lymphocytes, which are known to express moderate levels of telomerase [58]. Another explaination for telomerase activity in prostate tumor adjacent tissue, considering the relatively high levels and correlative (but reduced) levels with match PCa tissue, may be cancer field effects. Field cancerization in the prostate has been well documented [59,60] and telomerase activation in tumor-adjacent, histological

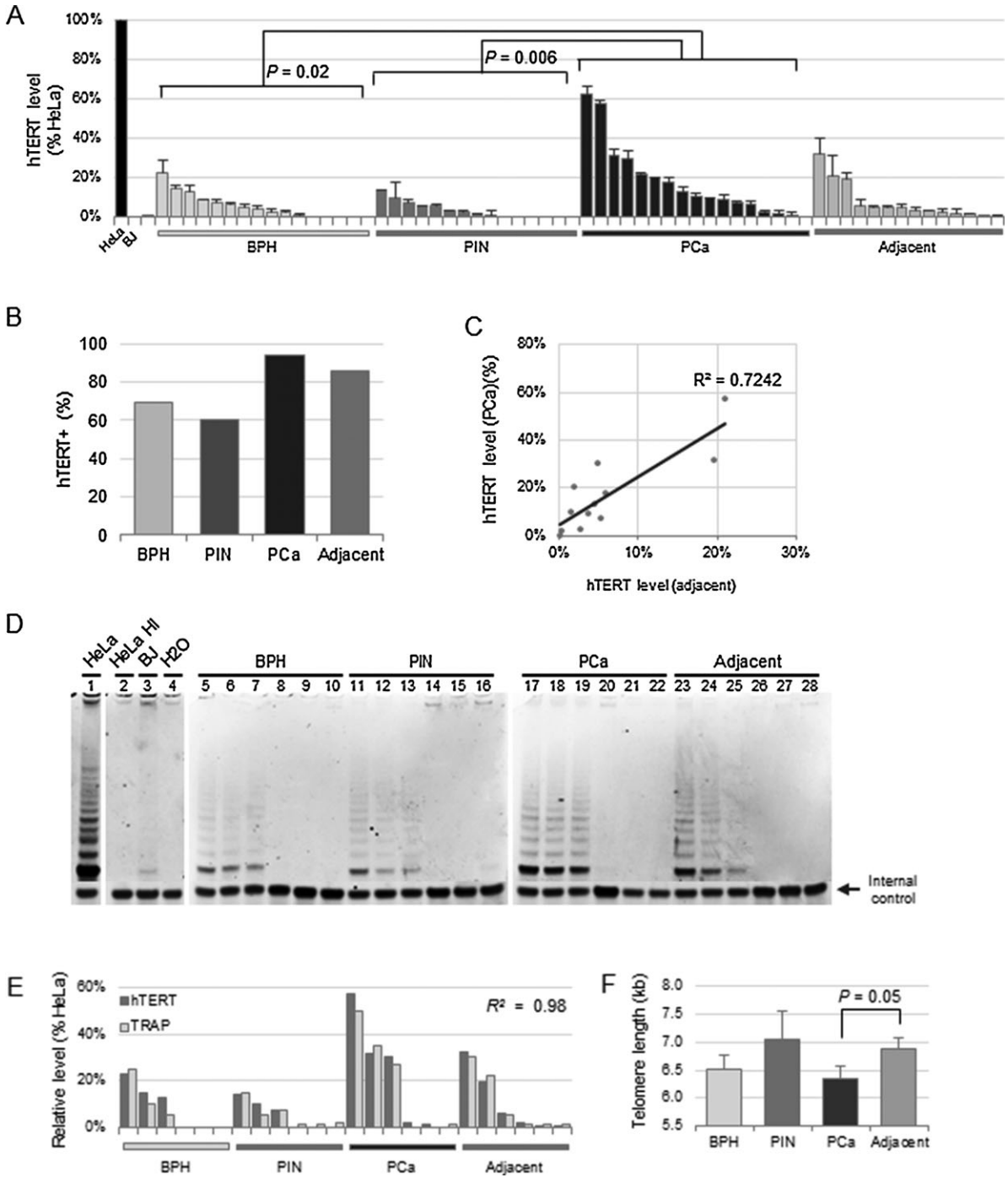

Figure 5. hTERT, telomerase, and telomere length profiles of each prostate tissue group. Benign prostatic hyperplasia (BPH), prostatic intraepithelial neoplasia (PIN), prostate cancer (PCa), and tumor adjacent, histologically normal adjacent (adjacent) prostate tissues. (A) hTERT expression levels in prostatic lesions normalized by the hTERT level in HeLa cells. Primary BJ fibroblast cells used as negative controls. Each bar represented the result from one individual tissue repeated four times (mean ± se). The sample sizes: BPH = 16, PIN = 15, PCa = 17, and tumor adjacent = 14. (B) Percentage of tissues positive for hTERT expression in each prostatic tissue. (C) Correlation of hTERT level between 15 PCa and the corresponding tumor adjacent, histologically normal (adjacent) ($R^2 = 0.72$). (D) Representative examples of telomerase activity in prostatic lesion samples. Three samples in each tissue type with the highest hTERT levels and three with non-detectable hTERT are shown. HeLa cells used as a positive control. Heat-inactivated HeLa (HeLa HI), BJ, and H_2O were used as negative controls. (E) Correlation between hTERT expression level and telomerase activity. Dark gray bars represent the hTERT level. Light grey bars marked the relative telomerase activity measured from above panel D ($R^2 = 0.98$). (F) Telomere length in prostatic lesion samples (mean ± se). Sample size equals eight for each prostate tissue group.

normal tissue has been reported in head and neck, and breast carcinogenesis [61].

Thus, telomere fusions are present in BPH and in the well-established early precursor prostate lesion PIN, and they are maintained at similar frequencies in malignant prostate tissues (PCa). Accumulating evidence suggests that telomere dysfunction is an early gateway event in the step-wise progression toward cancer and that telomere dysfunction may also drive cancer progression and intratumoral genetic heterogeneity via stochastic breakage fusion-bridge-cycles [24–26]. Telomere dysfunction driven genomic instability may be one of the most highly prevalent mechanisms of generating cancer-associated genetic aberrations in human carcinomas. Continuing studies of telomere dysfunction have the potential to identify new genetic candidate indicators of increased prostate cancer risk that may serve as important markers for detection and/or as targets for improved prevention and treatment strategies.

ACKNOWLEDGMENTS

This work was supported by grants to D.G. from the Indiana University Simon Cancer Center, the American Cancer Society, the Showalter Foundation, the Susan G. Komen Foundation, the Avon Foundation, the Flight Attendant Medical Research Institute, and the Indiana Genomics Initiative (INGEN). BG was supported by INGEN and the IU School of Medicine Division of Diagnostic Genomics. INGEN of Indiana University is supported in part by Lilly Endowment Inc.

REFERENCES

1. Palm W,de Lange T. How Shelterin Protects Mammalian Telomeres. Annu Rev Genet 2008;42:301–334.
2. Cifuentes-Rojas C, Shippen DE. Telomerase regulation. Mutat Res 2012;730:20–27.
3. Murnane JP. Telomere dysfunction and chromosome instability. Mutation research 2012;730:28–36.
4. Kannan N, Huda N, Tu L, et al. The luminal progenitor compartment of the normal human mammary gland constitutes a unique site of telomere dysfunction. Stem cell Reports 2013;1:28–37.
5. Artandi SE, DePinho RA. Telomeres and telomerase in cancer. Carcinogenesis 2010;31:9–18.
6. Genesca A, Pampalona J, Frias C, Dominguez D, Tusell L. Role of telomere dysfunction in genetic intratumor diversity. Adv Cancer Res 2011;112:11–41.
7. McClintock B. The stability of broken ends of chromosomes in Zea Mays. Genetics 1941;26:234–282.
8. Burrell RA, Swanton C. The evolution of the unstable cancer genome. Curr Opin Genet Dev 2013;24C:61–67.
9. Bostwick DG, Cheng L. Precursors of prostate cancer. Histopathology 2012;60:4–27.
10. Joshua AM, Evans A, Van der Kwast T, et al. Prostatic preneoplasia and beyond. Biochim Biophys Acta 2008;1785:156–181.
11. Tomlins SA, Mehra R, Rhodes DR, et al. Integrative molecular concept modeling of prostate cancer progression. Nat Genet 2007;39:41–51.
12. Bechis SK, Otsetov AG, Ge R, Olumi AF. Personalized medicine for management of benign prostatic hyperplasia. J Urol 2014;192:16–23.
13. Pavelic J, Zeljko Z, Bosnar MH. Molecular genetic aspects of prostate transition zone lesions. Urology 2003;62: 607–613.
14. Wadhera P. An introduction to acinar pressures in BPH and prostate cancer. Nat Rev Urol 2013;10:358–366.
15. Izumi K, Mizokami A, Lin WJ, Lai KP, Chang CS. Androgen receptor roles in the development of benign prostate hyperplasia. Am J Pathol 2013;182:1942–1949.
16. De Marzo AM, Nelson WG, Meeker AK, Coffey DS. Stem cell features of benign and malignant prostate epithelial cells. J Urol 1998;160:2381–2392.
17. McNeal JE, Redwine EA, Freiha FS, Stamey TA. Zonal distribution of prostatic adenocarcinoma. Correlation with histologic pattern and direction of spread. Am J Surg Pathol 1988;12:897–906.
18. Prakash K, Pirozzi G, Elashoff M, et al. Symptomatic and asymptomatic benign prostatic hyperplasia: Molecular differentiation by using microarrays. Proc Natl Acad Sci USA 2002;99:7598–7603.
19. Partin AW, Getzenberg RH, CarMichael MJ, et al. Nuclear matrix protein patterns in human benign prostatic hyperplasia and prostate cancer. Cancer Res 1993;53:744–746.
20. Zhang W, Kapusta LR, Slingerland JM, Klotz LH. Telomerase activity in prostate cancer, prostatic intraepithelial neoplasia, and benign prostatic epithelium. Cancer Res 1998;58: 619–621.
21. Sommerfeld HJ, Meeker AK, Piatyszek MA, Bova GS, Shay JW, Coffey DS. Telomerase activity: A prevalent marker of malignant human prostate tissue. Cancer Res 1996;56:218–222.
22. Paradis V, Dargere D, Laurendeau I, et al. Expression of the RNA component of human telomerase (hTR) in prostate cancer, prostatic intraepithelial neoplasia, and normal prostate tissue. J Pathol 1999;189:213–218.
23. Orsted DD, Bojesen SE. OPINION the link between benign prostatic hyperplasia and prostate cancer. Nat Rev Urol 2013;10:49–54.
24. Lin TT, Letsolo BT, Jones RE, et al. Telomere dysfunction and fusion during the progression of chronic lymphocytic leukemia: Evidence for a telomere crisis. Blood 2010;116: 1899–1907.
25. Roger L, Jones RE, Heppel NH, Williams GT, Sampson JR, Baird DM. Extensive telomere erosion in the initiation of colorectal adenomas and its association with chromosomal instability. J Natl Cancer Inst 2013;105:1202–1211.
26. Tanaka H, Abe S, Huda N, et al. Telomere fusions in early human breast carcinoma. Proc Natl Acad Sci USA 2012;109:14098–14103.
27. Zou Y, Misri S, Shay JW, Pandita TK, Wright WE. Altered states of telomere deprotection and the two-stage mechanism of replicative aging. Mol Cell Biol 2009;29:2390–2397.
28. Bhusari S, Yang B, Kueck J, Huang W, Jarrard DF. Insulin-like growth factor-2 (IGF2) loss of imprinting marks a field defect within human prostates containing cancer. Prostate 2011;71:1621–1630.
29. Yang B, Bhusari S, Kueck J, et al. Methylation profiling defines an extensive field defect in histologically normal prostate tissues associated with prostate cancer. Neoplasia 2013;15:399.
30. Livak KJ, Schmittgen TD. Analysis of relative gene expression data using real-time quantitative PCR and the 2(T)(-Delta Delta C) method. Methods 2001;25:402–408.
31. Huda N, Tanaka H, Herbert BS, Reed T, Gilley D. Shared environmental factors associated with telomere length maintenance in elderly male twins. Aging Cell 2007;6: 709–713.
32. Herbert BS, Hochreiter AE, Wright WE, Shay JW. Nonradioactive detection of telomerase activity using the telomeric

repeat amplification protocol. Nat Protoc 2006;1: 1583–1590.
33. Slee RB, Steiner CM, Herbert BS, et al. Cancer-associated alteration of pericentromeric heterochromatin may contribute to chromosome instability. Oncogene 2012;31: 3244–3253.
34. Takubo K, Fujita M, Izumiyama N, et al. Q-FISH analysis of telomere and chromosome instability in the oesophagus with and without squamous cell carcinoma in situ. J Pathol 2010;221:201–209.
35. Montgomery E, Wilentz RE, Argani P, et al. Analysis of anaphase figures in routine histologic sections distinguishes chromosomally unstable from chromosomally stable malignancies. Cancer Biol Ther 2003;2:248–252.
36. Acilan C, Potter DM, Saunders WS. DNA repair pathways involved in anaphase bridge formation. Genes Chromosomes Cancer 2007;46:522–531.
37. Luo J, Duggan DJ, Chen Y, et al. Human prostate cancer and benign prostatic hyperplasia: Molecular dissection by gene expression profiling. Cancer Res 2001;61:4683–4688.
38. Stamey TA, Warrington JA, Caldwell MC, et al. Molecular genetic profiling of Gleason grade 4/5 prostate cancers compared to benign prostatic hyperplasia. J Urol 2001;166:2171–2177.
39. Rhodes DR, Barrette TR, Rubin MA, Ghosh D, Chinnaiyan AM. Meta-analysis of microarrays: Interstudy validation of gene expression profiles reveals pathway dysregulation in prostate cancer. Cancer Res 2002;62:4427–4433.
40. Fromont G, Chene L, Latil A, et al. Molecular profiling of benign prostatic hyperplasia using a large scale real-time reverse transcriptase-polymerase chain reaction approach. J Urol 2004;172:1382–1385.
41. Alonso V, Neves AF, Marangoni K, et al. Gene expression profile in the peripheral blood of patients with prostate cancer and benign prostatic hyperplasia. Cancer Detect Prev 2009;32:336–337.
42. Shen MM, Abate-Shen C. Molecular genetics of prostate cancer: New prospects for old challenges. Genes Dev 2010;24:1967–2000.
43. Abate-Shen C, Shen MM. Molecular genetics of prostate cancer. Genes Dev 2000;14:2410–2434.
44. Navone NM, Troncoso P, Pisters LL, et al. P53 protein accumulation and gene mutation in the progression of human prostate carcinoma. J Natl Cancer Inst 1993;85: 1657–1669.
45. Kallakury BV, Figge J, Ross JS, Fisher HA, Figge HL, Jennings TA. Association of p53 immunoreactivity with high gleason tumor grade in prostatic adenocarcinoma. Hum Pathol 1994;25:92–97.
46. Thompson SJ, Mellon K, Charlton RG, Marsh C, Robinson M, Neal DE. P53 and Ki-67 immunoreactivity in human prostate cancer and benign hyperplasia. Brit J Urol 1992;69:609–613.
47. Luo J, Dunn T, Ewing C, et al. Gene expression signature of benign prostatic hyperplasia revealed by cDNA microarray analysis. Prostate 2002;51:189–200.
48. Djonov V, Ball RK, Graf S, et al. Transforming growth factor-beta 3 is expressed in nondividing basal epithelial cells in normal human prostate and benign prostatic hyperplasia, and is no longer detectable in prostate carcinoma. Prostate 1997;31:103–109.
49. Tapia-Laliena MA, Korzeniewski N, Hohenfellner M, Duensing S. High-risk prostate cancer: A disease of genomic instability. Urol Oncol 2014;32:1101–1107.
50. Vukovic B, Park PC, Al-Maghrabi J, et al. Evidence of multifocality of telomere erosion in high-grade prostatic intraepithelial neoplasia (HPIN) and concurrent carcinoma. Oncogene 2003;22:1978–1987.
51. Meeker AK, Hicks JL, Platz EA, et al. Telomere shortening is an early somatic DNA alteration in human prostate tumorigenesis. Cancer Res 2002;62:6405–6409.
52. Koeneman KS, Pan CX, Jin JK, et al. Telomerase activity, telomere length, and DNA ploidy in prostatic intraepithelial neoplasia (PIN). J Urology 1998;160:1533–1539.
53. Heaphy CM, Fleet TM, Treat EG, et al. Organ-wide telomeric status in diseased and disease-free prostatic tissues. Prostate 2010;70:1471–1479.
54. Joshua AM, Shen E, Yoshimoto M, et al. Topographical analysis of telomere length and correlation with genomic instability in whole mount prostatectomies. Prostate 2011;71:778–790.
55. Capper R, Britt-Compton B, Tankimanova M, et al. The nature of telomere fusion and a definition of the critical telomere length in human cells. Genes Dev 2007;21:2495–2508.
56. Bettendorf O, Heine B, Kneif S, et al. Expression-patterns of the RNA component (hTR) and the catalytic subunit (hTERT) of human telomerase in nonneoplastic prostate tissue, prostatic intraepithelial neoplasia, and prostate cancer. Prostate 2003;55:99–104.
57. Glybochko PV, Zezerov EG, Glukhov AI, et al. Telomerase as a tumor marker in diagnosis of prostatic intraepithelial neoplasia and prostate cancer. Prostate 2014;74:1043–1051.
58. Aubert G, Baerlocher GM, Vulto I, Poon SS, Lansdorp PM. Collapse of telomere homeostasis in hematopoietic cells caused by heterozygous mutations in telomerase genes. PLoS Genet 2012;8:1002696.
59. Rivenbark AG, Coleman WB. Field cancerization in mammary carcinogenesis-Implications for prevention and treatment of breast cancer. Exp Mol Pathol 2012;93:391–398.
60. Nonn L, Ananthanarayanan V, Gann PH. Evidence for field cancerization of the prostate. Prostate 2009;69: 1470–1479.
61. Patel MM, Patel DD, Parekh LJ, et al. Evaluation of telomerase activation in head and neck cancer. Oral oncology 1999;35:510–515.